Ch. 4: Water flow in soils

Table of Contents

4 Water flow in soils

4.1 Introduction

The water flow model simulates soil water content, soil water potential, vertical and, potentially, horizontal water flow in the soil, and water flow towards roots, biopores, and drains.

It is a basic assumption that water flow in the unsaturated zone can take place as Darcy flow within the soil matrix (calculated with Richard's equation (section 4.3) between numerical grid cells (section 4.10)) or as gravity flow in distinct macropores (biopore flow). Other forms of preferential flow, e.g., finger flow, are not considered. Hence, Daisy considers two flow regimes: a matrix regime (section 4.3) and a biopore regime (section 4.7). Additionally, matrix water can be divided into two subdomains to improve the description of the solute movement (chapter 6).

In this chapter, the build-up of a soil column is described first, as the column is a requirement for the hydraulic calculations. This is followed by a description of the processes included and the most used parameterisations available in Daisy. Particularly the number of hydraulic functions to describe retention curves and hydraulic conductivity is large and the ones not included in this chapter can be found in Appendix 4.1.

4.2 A soil column

A soil column can be either 1-dimensional (1D) or 2-dimensional (2D). In a 1D soil column only vertical water flow is simulated, whereas in a 2D soil column both vertical and horizontal water flow are simulated. The soil column extent from the soil surface (upper boundary, section4.4.1) and to a user defined depth (typically 2-3 meter below the soil surface), defining the exchange with groundwater (lower boundary, section4.4.2), see Figure 4.1.

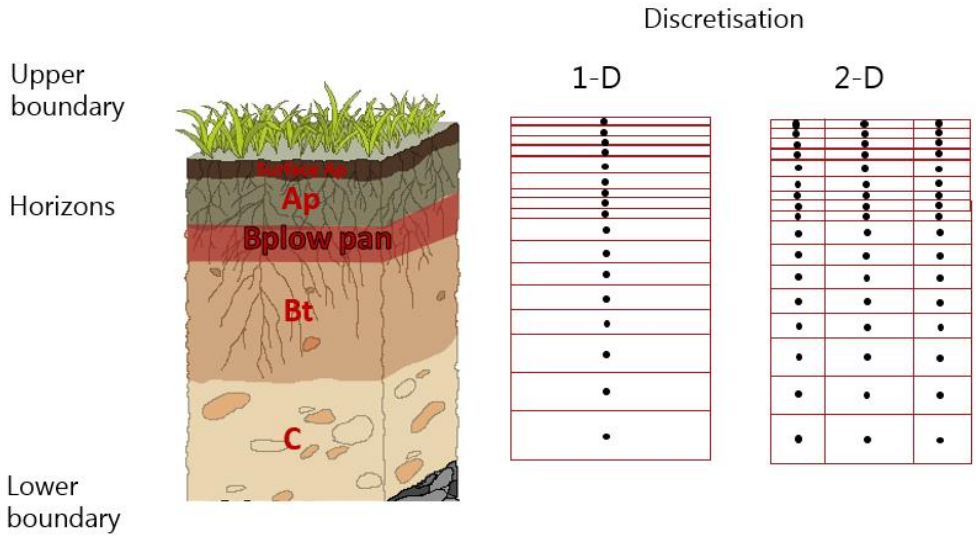

Figure 4.1. A soil column with horizons and examples of discretisation in 1 and 2 dimensions.

4.2.1 Soil horizons

The soil column consists of a user specified number of horizons (typically at least 3 e.g., an A-, B- and C-horizon). The start and end depth of the soil horizons are user defined. The properties of a soil horizon are considered homogeneous and static with regards to soil texture and hydraulic properties. The horizon has a range of properties required for calculating the flow of water, solute and heat, and the organic matter dynamics. For the water flow in soil, the most important properties are the soil texture, humus content, the dry bulk density, and the selected hydraulic process description with parameters (if the parameters are not generated by a pedotransfer function) (see section 4.5.1)). Please note, that there are many different systems for definition of soil texture, and it is important to know which one was used for the soils to be simulated. Daisy is able to handle the texture classification systems listed in Table 4.1.

Table 4.1: Textural classification schemes supported by Daisy. All numbers are µm.

Texture class/ Texture classification scheme	Clay	Silt			Sand				
		Fine	Medium	Coarse	Fine		Medium	Coarse	
					Very Fine	Fine		Coarse	Very Coarse
MIT3, DIN3, BSI3	<2	2-60			60-2000				
MIT7, BSI7	<2	2-6	60-200	20-60	60-200		200-600	600-2000	
DIN5	<2	2-60			60-200		200-600	600-2000	
ISSS3	<2	2-20			20-2000				
ISSS4	<2	2-20			20-200		200-2000		
FAO3, USDA3	<2	2-50			50-2000				
FAO7, USDA7	<2	2-50			50-100	100-250	250-500	500-1000	1000-2000
USPRA3	<5	5-50			50-2000				
USPRA4	<5	5-50			50-250		250-2000		

In addition to texture, the fraction of chalk can be specified, as well as the fraction of "*other*", typically larger mineral components (stones, pebbles). Daisy will ignore this fraction, but it can be included to ensure the sum is 1.0. The *normalize* parameter is by default *false,* but if set to *true* Daisy will normalize the mineral fractions of the soil to 1. The dry bulk density [g cm^{-3}] is calculated from the soil constituents based on the soil porosity and particle density of the specified soil particles, or can be specified by the user. If calculated, the assumed bulk density of minerals, humus and chalk are 2.65, 1.3 and 1.6 [g cm^{-3}], respectively (hard coded in texture.C).

4.2.2 Discretisation

The calculation of water flow in a 1D-column takes place between vertically aligned calculation nodes (Figure 4.1), which are the centre points of grid cells, and only vertical gradients are simulated. For 2D-simulations, grid cells with calculation nodes must be defined in both vertical and horizontal direction.

Manual discretisation

The discretization can be user defined. In the 1D-column, it is defined with the array z_{plus} [cm], while the discretization of the 2D soil column must be user specified with the arrays z_{plus} [cm] and x_{plus} [cm]. The specification is done using the *Geometry* function, from top to bottom and left to right, respectively.

Automatic discretisation

For the 1D-column, the user can also choose to let the model create a discretization. The automatic discretization is guided by several rules:

- There must be a division at each soil horizon boundary and for each specified boundary for logging.
- A horizon should preferably be divided into three calculation layers (but the automatic scheme gives an error message if layers become less than 1 cm high).
- For cells with the top between 0 and 5 cm depth, the default cell height is 2.5 cm.
- For cells with the top between 5 and 10 cm, the default cell height is 5 cm.
- For cells with the top between 10 cm and (rooting depth-50 cm), the default cell height is 10 cm.
- Below this depth, the default cell height is 20 cm, but this is generally overruled by a maximum cell height of "2*dispersivity", as the default value for dispersivity is 5 cm.
- If the space between fixed boundaries does not allow cells of the default size, the cells are reduced to fit the size.

Except in the top layers, integer values for depth are used, as far as possible. The result of the automatic discretisation is recorded in the Daisy logfile.

4.3 Water flow in the matrix soil

It is a basic assumption in Daisy that water flow in the unsaturated zone can take place as Darcy flow within the soil matrix or as gravity flow in distinct macropores. Water flow in the soil matrix is described with Richards equation (Richards, 1931), both in 1D (eq. 1) and 2D (eq. 3):

Richards Equation 1D

$$\frac{\partial \theta}{\partial t} = \frac{\partial}{\partial z}\left(K_z(h)\frac{\partial h}{\partial z}\right) + \Gamma_{RWU} + \Gamma_{DF} + \Gamma_{BF} \qquad (1)$$

where

θ = the volumetric water content [$cm^3\ cm^{-3}$]

t = time [h]

z = the vertical spatial coordinate

h = pressure head [cm]

K_z = the hydraulic conductivity in the z-direction as a function of h [$cm\ h^{-1}$], and

$\Gamma_{RWU}, \Gamma_{DF}$ and Γ_{BF} [$cm^3\ cm^{-3}\ h^{-1}$] are source-sink terms representing root water uptake (RWU, section4.8), drain water flow (DF, section4.6) and biopore water flow (BF, section4.7), respectively.

A solution to Richard's equation requires knowledge of a relation between θ and h, i.e. a soil water characteristic or retention curve, and knowledge of the relation between K and h or θ, i.e. the hydraulic conductivity function. Several models for these relations have been proposed in literature and several of these are available as submodels in Daisy, see section 4.5 and Appendix 4.1.

Richard's equation is solved numerically in the mixed formulation (Celia et al., 1990), see section 4.10. The upper boundary condition is determined internally by Daisy (see section 4.4.1 and Chapter 3). It may be constituted by a pressure condition when ponding occurs, or a flux condition in all other circumstances. The lower boundary is selected by the user (section 4.4.2. The following conditions are implemented: a pressure condition (known position of the groundwater), gravity flow (deep groundwater), and a lysimeter boundary condition. A special case of a pressure condition is implemented, viz. a pipe drain condition (see below).

lr model

If the numeric solution to Richards Eq. does not converge within a specified number of iterations, a simplified model is used. In the simplified model (termed *lr* in Daisy) water movement (both upwards and downwards) down to *z_top* (default -10 [cm]) is calculated with the Darcy Equation:

$$q = -K_z\left(\frac{\partial h}{\partial z} + 1\right) \tag{2}$$

Below *z_top* only gravitational water movement in wet soil is accounted for. Wet soil is defined as soil with a pressure head above field capacity (termed *h_fc* in Daisy with a default of -100 cm).

Richards Equation 2D

Richards Equation in 2D considers both vertical (z-direction) and horizontal (x-direction) water flow:

$$\frac{\partial \theta}{\partial t} = \nabla \cdot \left(\boldsymbol{K}(h)\nabla(h+z)\right) + \Gamma_{RWU} + \Gamma_{DF} + \Gamma_{BF} \tag{3}$$

where $\boldsymbol{K}(h)$ is the hydraulic conductivity tensor, and h is the potential head. The x-axis is chosen in horizontal direction and the z-axis is positive upwards. The conductivity tensor can be expressed as:

$$\boldsymbol{K} = \begin{bmatrix} K_{xx} & K_{xz} \\ K_{zx} & K_{zz} \end{bmatrix}$$

For a model with rectangular cells, we have chosen that the principal directions of the anisotropic medium are parallel to the x- and z-axis, i.e.

$$\boldsymbol{K} = \begin{bmatrix} K_{xx} & 0 \\ 0 & K_{zz} \end{bmatrix}$$

The hydraulic conductivities have the unit [cm h^{-1}].

The 2D Richard's Equation (Eq. 3) is solved numerically with a finite volume solution (Mollerup and Hansen, 2007) (section 4.10). If the numeric solution to the equation does not converge within the prescribed number of iterations, the

model issues a warning and adopts a simplified water model ($v+h$). If the $v+h$-model does not converge a steady-state water flow model (*const*) is applied.

v+h model

In the $v+h$-model, water flow is, in principle, calculated in two steps, first vertically and then horizontally. However, the default setting for horizontal water flow in the *v+h*-model is none. Vertical water flow is then calculated with the 1D Richards Equation (Eq. 1).

const model

In the steady-state water flow model *const* a constant water flow in horizontal and vertical direction is assumed. The flow is defined by q_x [cm h^{-1}] and q_z [cm h^{-1}], both with default values of 0. The sink terms are, however, still active in both models.

4.4 Boundary conditions

The characteristics of the boundaries of the simulated domain in Daisy vary depending on their position.

Side boundaries: No flow

The side-boundaries are defined as no-flow boundaries, whereas the top boundary is defined by the surface processes (Chapter 3) and the bottom boundary can be defined with either free drainage, a fixed or fluctuating groundwater table or pressure, an aquitard, or a lysimeter boundary.

4.4.1 The top boundary

The upper boundary condition depends on the conditions at the surface (Chapter 3). The three following situations are implemented:

- A specified flux in or out of the soil surface (Neuman condition)
- A specified potential at the soil surface (Dirichlet condition)
- A specified flux at a specified depth (Neuman condition)

Specified flux at soil surface (Neuman condition)

The first boundary condition specified is used when rain, irrigation or melting snow causes infiltration that does not exceed the infiltrability of the soil (downwards) or when evaporation takes place from the surface (upwards, section 3.3). If the amount of water available for infiltration is positive, but less than the infiltrability of the soil, the amount of available water determines the flux. If no water is available for infiltration, the dominating process is evaporation. The actual soil evaporation is either given by the potential evaporation from the soil surface [mm h^{-1}] or by the rate at which soil water can be transported to the soil surface, $J_{w,Soil\_exf}$ [mm h^{-1}] (Eq. 3.38). The soil exfiltration rate is determined as:

$$J_{w,Soil\_exf} = \frac{K}{C_\theta}\left[\frac{\partial\theta}{\partial z}\right]_{z=0} \quad (4)$$

where:

K = the hydraulic conductivity of the soil

C_θ = the specific water capacity $= \frac{d\theta}{dh}$ and

The gradient $\frac{\partial\theta}{\partial h}$ is estimated on the assumption that $\theta = 0$ at $z = 0$.

Specified potential at soil surface (Dirichlet condition)

The second boundary condition specified is used when water is ponding on the soil surface (section 3.2.4). This may occur when rain, irrigation or melting snow provides water at a rate which exceeds the infiltrability of the soil.

Specified flux in soil profile (Neuman condition)

The third top boundary condition specified is used when Richards Equation (Eq. 1 and 33) is not solved for the whole profile. This is often the case when freezing or thawing takes place (section 4.9).

4.4.2 The lower boundary

The lower boundary can be defined with one of the four following conditions:

- Free drainage,
- A groundwater level at constant or varying depth,
- A specified flux at a specified depth
- An aquitard in combination with a pressure potential at a specified depth.
- A lysimeter boundary (seepage face type)

Free drainage

Free drainage is applied by selecting the "deep" option in Daisy. In this case, the flux is equal to the hydraulic conductivity defined by the moisture content of the lowest cell. The total hydraulic head gradient is equal to 1. This is also called gravitational flow.

Groundwater depth

A groundwater depth may be used when the position of the groundwater is known. A constant ground water table is defined with the model *fixed* as a negative number below surface. A dynamic groundwater table can be read from a file including information of year, month, day, and groundwater height as negative numbers below surface. Linear interpolation is used between the datapoints.

Flux as a specified depth

A specified flux at a specified depth can be simulated by applying the *flux* groundwater model. With the *flux* model a constant flux to the groundwater is simulated.

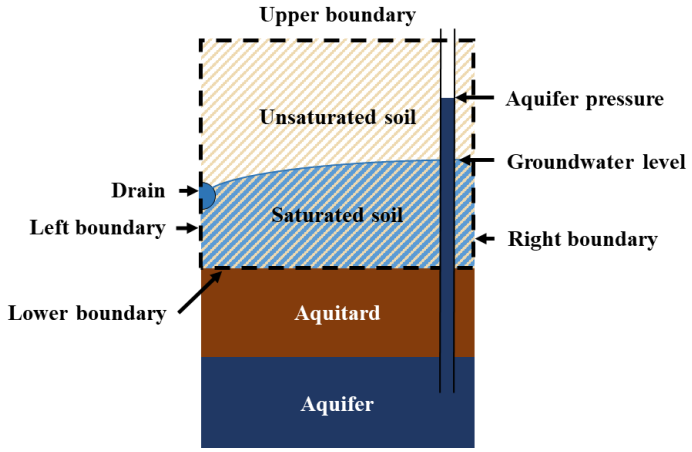

Figure 4.2: Schematic representation of the aquitard boundary. Modified from Hansen et al. (2012).

Aquitard

The aquitard boundary condition allows for both upwards and downwards fluxes of water through the aquitard. The water flux over the aquitard is calculated as:

$$q_a = K_a \frac{h_p - h_a}{\Delta z_a} \quad (5)$$

where:

K_a = the hydraulic conductivity of the aquitard [cm h^{-1}]

Δz_a = the height of the aquitard [cm]

h_a = the pressure potential in the aquifer at the interphase between the aquitard and the aquifer [cm] (specified as static or dynamic (file), and

h_p = the pressure head of the last node in the soil column [cm]

Aquitard and drain pipes

The aquitard option is commonly used in combination with simulation of drain pipes, see section 4.6.

Lysimeter boundary

The lysimeter boundary describes a system where saturation, or build up of a positive pressure, is required before water will leave the lowest calculation node of the column. The flow is determined by the saturated hydraulic conductivity and the positive pressure, as the pressure below the column is assumed to be air pressure.

4.5 Hydraulic parameter-functions (HPFs) available in Daisy

As mentioned above, water calculations require that soil hydraulic properties for each horizon are defined by the soil water retention curve, describing the relation between soil water content, θ and soil water pressure, h, as well as the hydraulic conductivity curve, describing the relation between the hydraulic conductivity, K, and h.

In the following, some of the simple, well known hydraulic submodels (the Brooks and Corey (Brooks and Corey, 1964) and the Campbell (Campbell, 1974) retention curves in combination with Burdine or Mualem theory, and the Van Genuchten retention curve (Van Genuchten, 1980) in combination with Burdine (Burdine, 1953), Mualem (Mualem, 1976)) are described, together with pedotransfer-functions providing the required parameters. In Appendix 4.1, the rest of the available options are described. This includes the Brunschwick version of the van Genuchten retention curve model with Mualem and Tokunga theory for hydraulic conductivity (Tokunaga, 2009), (Weber et al., 2019) as well as a range of bimodal submodels, tabulated curves, and attempts to include changes over time, such as hysteresis and tillage The possibility to supply Daisy with the soil hydraulic properties in a tabular form makes it possible to use any model for the SHPs. It should also be noted that the architecture of the Daisy code makes it relatively easy to add new hydraulic models.

Classical soil water retention curves

The expressions for the retention curves developed by Brooks and Corey (1964), Campbell (1974), Van Genuchten (1980), and the modified Campbell curve (Smith, 1992) are shown in Table 4.2 with the following notation:

S_e = effective soil water content [-].

S_r = relative soil water content [-].

θ_s = volumetric soil water content at saturation [$cm^3\ cm^{-3}$].

θ_r = residual volumetric soil water content [$cm^3\ cm^{-3}$].

h_b = bubling pressure, air-entry value [cm],

h = pressure [cm], and

λ [-], b [-], α [cm^{-1}] and n [-] are shape parameters (pore size index).

Lastly, it is assumed that $m = 1 - \frac{1}{n}$

Table 4.2: The Brooks and Corey, Campbell, and van Genuchten mathematical descriptions of the soil water retention curve.

Reference	Mathematical form	Condition	Eq. nr.
Brooks and Corey (1964)	$S_e = \frac{\theta - \theta_r}{\theta_s - \theta_r} = \left(\frac{h_b}{h}\right)^{\lambda}$	$h_p < h_b$	(6)
Campbell (1974)	$S_r = \frac{\theta}{\theta_s} = \left(\frac{h_b}{h}\right)^{\frac{1}{b}}$	$h_p < h_b$	(7)
Modified Campbell	$S_r = \left(\frac{\theta}{\theta_s}\right) = \left(\frac{1}{\left(1 + \left(\frac{h}{h_b}\right)^5\right)^{5b}}\right)$	$h_p < h_b$	(8)
Van Genuchten (1980)	$S_e = \frac{\theta - \theta_r}{\theta_s - \theta_r} = \left[\frac{1}{1 + \lvert\alpha h\rvert^n}\right]^m$	$h_p < 0$	(9)

The description of the soil water retention curves is combined with either Burdine or Mualem theory for hydraulic conductivity, see Table 4.3. The Burdine form parameter is 2 by default, while the Mualem form parameter is 0.5. However, these defaults can be changed, if required, by substituting the *"l"*-values of 2 or 0.5 with a different value. The exponent in the Brooks and Corey/Burdine-hydraulic conductivity calculation: $p=(2+3\lambda)/\lambda$ can also be written as $p=2/\lambda+(\text{"}l\text{"}+1)$, while the exponent for the Mualem solution can be written as: $p=(2+2.5\lambda)/\lambda$ or $p=2/\lambda+(\text{"}l\text{"}+2)$. For the Campbell hydraulic functions, λ is exchanged with $1/b$.

For the hydraulic conductivity equations built on van Genuchten retention curves, the *"l"*-values of 2 or 0.5 are exponents on S_e in equation 9 and 10 below.

The equations below all show K as a function of K_s, but alternatively, a K at a specified pressure (h) can be given as input.

Anisotropy

For all the hydraulic conductivity models, the saturated hydraulic conductivity [cm h^{-1}] in the horizontal direction ($K_{s,xx}$) can be scaled relative to the vertical direction ($K_{s,zz}$) applying an *anisotropy* [-] factor. The *anisotropy* factor is by default 1, thus K_s is, by default, equally in the horizontal and vertical direction. Otherwise, ($K_{s,xx}$) = ($K_{s,zz}$) *anisotropy*.

Table 4.3. Expressions for unsaturated hydraulic conductivity as function of saturated hydraulic conductivity, K_s [cm h^{-1}] and the selected retention curve.

Retention curve	Theory	Daisy model name	Equation	Eq. Nr
Brooks and Corey	Burdine	B_BaC	$K = K_s S_e^{(2+3\lambda)/\lambda}$	(10)
	Mualem	M_BaC	$K = K_s S_e^{(2+2.5\lambda)/\lambda}$	(11)
Campbell	Burdine	B_C	$K = K_s S_r^{(2+3/b)b}$	(12)
	Mualem	M_C	$K = K_s S_r^{(2+2.5/b)b}$	(13)
Van Genuchten	Burdine	B_vG	$K = K_s S_e^2 \left[1 - \left(1 - S_e^{\frac{1}{m}}\right)^m\right]$ $m = 1 - \frac{2}{n}$	(14)
	Mualem	M_vG	$K = K_s S_e^{\frac{1}{2}} \left[1 - \left(1 - S_e^{\frac{1}{m}}\right)^m\right]^2$ $m = 1 - \frac{1}{n}$	(15)

4.5.1 Pedotransferfunctions for HPFs

Three pedotransfer functions (PTFs) for generation of soil hydraulic properties from other soil properties, such as texture and bulk density, are implemented in Daisy: Cosby (Cosby et al., 1984), HYPRES (Wösten et al., 1998) and Hypweb (Weber et al., 2020). Hypweb is described in Appendix 4.1.

Cosby PFT

The Cosby PTF generates the parameters θ_s, k_s, h_b and b for the modified Campbell retention curve (Eq. 4.8) and the Campbell-Burdine hydraulic conductivity curve (Eq. 4.12) based on the clay, silt, and sand [%] fractions:

$$\theta^*(h) = 0.505 - 0.00142 * Sa - 0.00037 * Cl \quad (16)$$

$$\log_{10}(h_b) = 1.54 - 0.0095 * Sa + 0.0063 * Si \quad (17)$$

$$\frac{1}{b} = 3.1 + 0.157 * Cl - 0.003 * Sa \quad (18)$$

$$\log_{10}(K_s) = -5.71 + 0.0126 * Sa - 0.0064 * Cl \quad (19)$$

where:

Cl = Clay fraction (< 2 µm) [%],

Si = Silt fraction (2-50 µm) [%], and

Sa = Sand fraction (50-2000 µm) [%].

h_b is in [cm water column] and K_s is in [m s^{-1}].

The Cobys PTFs are derived based on 1448 soil samples covering a wide variety of soil properties.

HYPRES PTF

The HYPRES PTF generates the parameters, θ_s, k_s, α, n and l, for the van Genuchten-Mualem retention curve and hydraulic conductivity curve (Eq. 4.9 and 4.15) based on clay, silt, organic matter, bulk density and a distinguishes between top- and subsoil. The HYPRES PTFs are based on 1777 sample locations with data from 4486 soil horizons in Europe. The R^2 below the equations express the fit between the established pedotransfer function and the measured data.

$$\begin{aligned}\theta_s = {} & 0.7919 + 0.001691 \cdot Cl - 0.29619 \cdot D - 0.000001491 \cdot Si^2 \\ & - 0.0000821 \cdot OM^2 + 0.02427 * Cl^{-1} + 0.01113 \\ & \cdot Si^{-1} + 0.01472 \\ & \cdot \ln(Si) - 0.0000733 \cdot OM \cdot Cl - 0.000619 \cdot D \cdot Cl \\ & - 0.001183 \cdot D \cdot OM - 0.0001664 \cdot topsoil \cdot Si \\ & (R^2 = 76\%)\end{aligned} \quad (20)$$

$$\begin{aligned}K_s^* = {} & 7.755 + 0.0352 \cdot Si + 0.93 \cdot topsoil - 0.967 \cdot D^2 \\ & - 0.000484 \cdot Cl^2 - 0.000322 \cdot Si^2 + 0.001 \cdot Si^{-1} \\ & - 0.0748 \cdot OM^{-1} - 0.643 \cdot \ln(Si) - 0.01398 \cdot D \cdot Cl \\ & - 0.1673 * D \cdot OM + 0.02986 \cdot topsoil \cdot Cl \\ & - 0.03305 \cdot topsoil \cdot Si \\ K_s = {} & e^{K_s^*} \qquad (R^2 = 19\%)\end{aligned} \quad (21)$$

$$\begin{aligned}\alpha^* = {} & -14.96 + 0.03135 \cdot Cl + 0.0351 \cdot Si + 0.646 \cdot OM + 15.29 \cdot D \\ & - 0.192 \cdot topsoil - 4.671 \cdot D^2 - 0.000781 \cdot Cl^2 \\ & - 0.00687 \cdot OM^2 + 0.0449 \cdot OM^{-1} + 0.0663 \\ & \cdot \ln(Si) + 0.1482 \cdot \ln(OM) - 0.04546 \cdot D \cdot Si \\ & - 0.4852 \cdot D \cdot OM + 0.00673 \cdot topsoil \cdot Cl \\ \alpha = {} & e^{\alpha^*} \qquad (R^2 = 20\%)\end{aligned} \quad (22)$$

$$
\begin{aligned}
n^* = {} & -25.23 - 0.02195 \cdot Cl + 0.0074 \cdot Si - 0.1940 \cdot OM + 45.5 \cdot D \\
& - 7.24 \cdot D^2 + 0.0003658 \cdot Cl^2 + 0.002885 \cdot OM^2 \\
& - 12.81 \cdot D^{-1} - 0.1524 \cdot Si^{-1} - 0.01958 \cdot OM^{-1} \\
& - 0.2876 \cdot \ln(Si) - 0.0709 \cdot \ln(OM) - 44.6 \cdot \ln(D) \\
& - 0.02264 \cdot D \cdot Cl + 0.0896 \cdot D \cdot OM + 0.00718 \\
& \cdot topsoil \cdot Cl \\
n = {} & e^{n^*} + 1 \qquad (R^2 = 54\%)
\end{aligned}
\tag{23}
$$

$$
\begin{aligned}
l^* = {} & 0.0202 + 0.0006193 \cdot Cl^2 - 0.001136 \cdot OM^2 - 0.2316 \\
& \cdot \ln(OM) - 0.03544 \cdot D \cdot Cl + 0.00283 \cdot D \cdot Si \\
& + 0.0488 \cdot D \cdot OM \\
l = {} & 10 \cdot \frac{(e^{l^*} - 1)}{(1 + e^{l^*})} \qquad (R^* = 12\%)
\end{aligned}
\tag{24}
$$

where:

Cl = clay (< 2 µm) [%]

Si = silt (0-50 µm) [%]

OM = Organic matter [%]

D = Bulk density [g cm^{-3}]

K_s is calculated in [cm d^{-1}], α is in [cm^{-1}]

Topsoil and *subsoil* are qualitative parameters having a value of 1 or 0, respectively.

4.6 Water flow to drains

Waterflow towards drains is calculated with Hooghoudts drainage equation (Hooghoudt, 1940) in 1D and with a dynamic drainage model in 2D (Mollerup et al., 2014).

Hooghoudts drainage equation

Hooghoudt's equation is based on several assumptions: Darcy's law should be valid for the water flow, and the soil should be homogeneous, with the specified hydraulic conductivities (K_1 and K_2). An impermeable layer (aquitard) underlies the drain at the depth D. The hydraulic gradient at any point is equal to the slope of the water table above the point. Recharge, as well as a water depth above the drain level in the radial flow zone is neglected.

In 1D, when the groundwater table is located above the drain depth, drain flow is estimated as:

$$
q_e = \frac{4K_1H^2 + 2K_2HD}{L\Delta x - \Delta x^2} \tag{25}
$$

where:

q_e = an equilibrium drain flow [cm m^2 m^{-2} h^{-1}] = [cm h^{-1}],

K_1 = hydraulic conductivity of the saturated soil above drain depth [cm h^{-1}],

K_2 = hydraulic conductivity of the saturated soil between drain depth and the aquitard (section 4.4.2),

L = the horizontal distance between the drains (default: 1800 [cm])

Δx = the horizontal distance between the simulated soil column and the drain [cm],

H = the vertical distance between the drain and the groundwater table [cm] and

D = is the vertical distance between the drain and the aquitard [cm]. In reality, D is substituted by an "equlibrium depth", which is close to D when D is small and less than D, when D is large. Daisy has three models for calculation of D, the default being *MolenWesseling* (van der Molen and Wesseling, 1991). For other options, see Appendix 4.2.

K_1 and K_2 is estimated as a weight-average of the hydraulic conductivities of saturated soil horizons above and below the drain, respectively, calculated as:

$$K_1 = \frac{\sum_{i=0}^{N} f_{1,i} \Delta z_i K_{s,i}}{H} \tag{26}$$

$$K_2 = \frac{\sum_{i=0}^{N} f_{2,i} \Delta z_i K_{s,i}}{D} \tag{27}$$

where:

N = number of numerical layers,

$K_{s,i}$ = the saturated conductivity of layer i,

Δz_i = the depth of cell i and

$f_{1,i}$ and $f_{2,i}$ = the saturated fraction of cell i above and below the drain respectively.

The equivalent depth (van der Molen and Wesseling, 1991) is calculated stepwise, as shown below:

$$y = \frac{2\pi D}{L} \tag{28}$$

$$y < 0.5 \Rightarrow \quad F(y) = \frac{\pi^2}{4y} + \ln\left(\frac{y}{2\pi}\right) \tag{29}$$

$$y \geq 0.5 \Rightarrow \quad F(y) = \frac{4e^{-2y}}{1(1-e^{-2y})} + \frac{4e^{-6y}}{3(1-e^{-6y})} + \frac{4e^{-10y}}{5(1-e^{-10y})} + \frac{4e^{-14y}}{7(1-e^{-14y})} + \frac{4e^{-18y}}{9(1-e^{-18y})} + \cdots. \tag{30}$$

$$De = \frac{\pi L}{8\left(F(y) + ln\left(\frac{L}{\pi r}\right)\right)} \tag{31}$$

r in the last equation is the radius of the drainpipe [cm].

The drain option is used with the aquitard boundary condition. It can also be used to simulate natural drain lines in the landscape, in which case L is much larger than the default value.

Dynamic drainage model

Drain water flow in 2D is simulated with a dynamic drainage model assuming atmospheric pressure (h=0) in the drain cell (Mollerup et al., 2014). Thus, when pressure in the surrounding soil increases above saturation $(h \geq 0)$, the pressure in the drain is forced to zero. Water flow to the drain is based on Richard's equation (Eq. 3) and all water flow to drains (both from matrix and through biopores (section 4.7) is instantaneously removed from the system, as drains are assumed to have an infinite capacity for removing soil water. When the pressure in the surrounding soil is below saturation $(h < 0)$, the pressure in the drain cell is simulated as for the surrounding soil.

4.7 Water flow to biopores

Daisy allows for an advanced and a simple description of biopores, which is also called the tertiary domain. The advanced model is described first.

Tertiary domain, biopores

Biopores in Daisy are simulated as vertically oriented cylindrical tubes, connecting the surface or topsoil with drains and/or deeper soil layers. The biopore geometry is characterized by a radius, r_b, and the depth where the biopore starts, z_b^{top}, and ends, z_b^{bot}, Figure 4.3. Further, the biopores are described as classes of biopores with the same geometry and a specified density, $D_b(i)$ [m^2], where i refers to the pore class. A column can comprise multiple biopore classes. In a 2D domain, specific biopore classes can be restricted to certain areas.

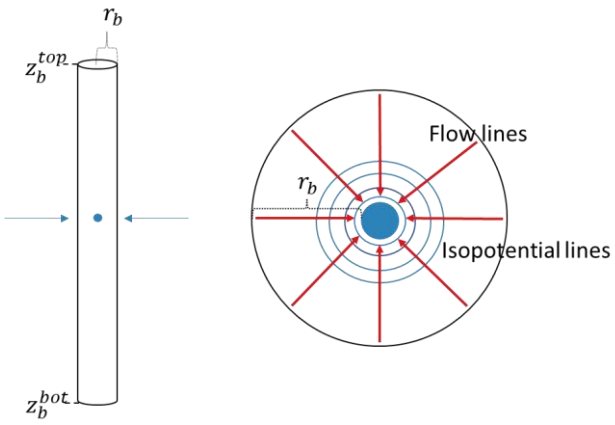

Figure 4.3: Radial water flow from the matrix to a biopore, modified from Holbak et al. (2021)

Pressure distribution in biopores

The pressure head distribution, h_b, inside the biopore is assumed to be in hydrostatic equilibrium and is a function of the water level inside the biopore. However, $h_b(z)$ never drops below h_{term}, which is the threshold value for termination of water movement from the matrix to the biopores (Holbak et al., 2021; Tofteng et al., 2002). Thus, $h_b(z)$ has a linear distribution between z_b^{bot} and h_{term}, with 0 at the bottom for empty biopores and 0 at the water level for partially filled biopores:

$$h_b(z) = \begin{cases} z_0 - z & if\ z_0 - z < h_{term} \\ h_{term} & if\ z_0 - z > h_{term} \end{cases} \quad (32)$$

where:

z_0 = water level in the biopore [cm]. For biopores connected to the drainpipe z_0 is equal to drain depth (section 4.6),

h_{term} = the termination threshold for water moving from the matrix to the biopore, by default – 30 [cm], and

z = the vertical coordinate (0 at the surface and negative downwards) [cm].

Infiltration from surface

For all biopores starting at the soil surface, $z_b^{top} = 0$, the amount of water infiltrating to the biopore from a ponding water layer, $q_{Pond,inf}^b$, (section 3.2.4) is calculated as:

$$q_{Pond,inf}^b = \begin{cases} 0, & P \le q_{Pond,inf}^m \\ P - q_{Pond,inf}^m, & P > q_{Pond,inf}^m \; and \; P - q_{Pond,inf}^m < q_{Pond,inf}^{b,max} \\ q_{Pond,inf}^{b,max}, & P - q_{Pond,inf}^m > q_{Pond,inf}^{b,max} \end{cases} \quad (33)$$

where:

P = precipitation [cm h^{-1}],

$q_{Pond,inf}^m$ = infiltration to the soil matrix [cm h^{-1}], and

$q_{Pond,inf}^{b,max}$ = the maximum allowed infiltration rate [cm h^{-1}] for a specific biopore approximated by Poiseuille's law assuming only gravity as the driving force:

$$q_{Pond,inf}^{b,max} = \frac{\pi r_b^4 \rho_w g (z_0 + H_{Pond})}{8 z_0 \mu A_b} \quad (34)$$

where:

ρ_w = density of water [g cm^{-3}],

g = the acceleration of gravity [cm h^{-2}],

H_{Pond} = the height of the ponding layer [cm],

μ = the dynamic viscosity [g cm^{-1} h^{-1}], and

A_b = area of the biopore [cm^2].

Waterflow from matrix to biopores

Waterflow from the matrix soil to biopores is activated when the soil matrix is at or very close to saturation, at h_{init}, by default = -3 [cm]. It continues until the pressure head in the matrix soil drops below the termination threshold, h_{term}. However, to secure numerical stability, a certain pressure difference between h and h_b must be exceeded. By default, this is set to 5 cm (the *pressure_barrier* parameter).

When calculating the flow from matrix to biopore, the total density of macropores ($D_{b,c}$) is considered and $r_{c,mean}$ is the average radius of the area supplying water to a given pore.

Waterflow from the matrix to the biopore is described as cylindrical symmetrical flow at a given depth, z_b (Figure 4.3). For each biopore class the waterflow over the matrix biopore interface is calculated as:

$$\Gamma_{BF}^{BC_i} = \frac{2\pi D_{b,c} K_x(h)\big(h(z) - h^b(z)\big)}{\ln\big(r_{c,mean}/r_b\big)} \tag{35}$$

where:

$D_{b,c}$ = density in the horizontal plane of biopores assuming the biopores are equidistantly placed [cm^{-2}],

$K_x(h)$ = the hydraulic conductivity in the x-direction as a function of h [cm h^{-1}],

r_b = radius of the biopores [cm],

h_b = pressure in the biopore [cm], and

h = pressure in the soil matrix [cm].

As $D_{b,c} \approx 1/(\pi \cdot r^2_{c,mean})$, this can be re-written to:

$$\Gamma_{BF}^{BC_i} = \frac{4\pi D_{b,c} K_x(h)\big(h^b(z) - h(z)\big)}{\ln\big(D_{b,c}\pi r_b^2\big)} \tag{36}$$

For calculating the combined biopore sink/source term in Richards Equation (Eq. 1 and 3) the sink/source terms for all biopore classes are summed:

$$\Gamma_{Bf} = \sum_{i=1}^{NC} \Gamma_{BF}^{BC_i} \tag{37}$$

where NC is the number of all biopore classes.

Water flow from biopore to matrix

The hydraulic conductivity of the biopore wall may be different (lower) than the conductivity of the soil matrix due to accumulation of clay and organic matter. This can be considered by applying a relative conductivity of the wall, K_w. r_w is the radius of the outer biopore wall, and r_w/r_b is set to 1.1. The flow from the biopore to the matrix can be described as:

$$\Gamma_{b\_m} = \frac{2\pi D_b(i) * K_x(h)\big(h_b(z) - h(z)\big)}{ln\left(\frac{r_m}{r_b}\right) - ln\left(\frac{r_w}{r_b}\right)} \cdot \frac{a}{1+a} \tag{38}$$

where

$$r_m \approx \sqrt{\frac{1}{\pi D_b(i)}}$$

$$a = K_w \cdot \frac{\left(ln \frac{r_m}{r_b} - ln\left(\frac{r_w}{r_b}\right)\right)}{ln\left(\frac{r_w}{r_b}\right)}$$

Instantanous water movement in biopores

Water movement in the biopores is assumed to be instantaneous. Thus, water flowing into a matrix-terminating biopore is added directly to the bottom of the biopore, or if the biopore is partly filled, to the top of the water level. Water flowing into a drain-connected biopore is assumed to instantaneously move to the drain and is thus directly removed from the system (section 4.6).

No macropores included

Macropore transport can be avoided using the command (tertiary none).

Default macropore model

The first macropore model <*old*> is still available in Daisy and works as default. The sub-module requires a distribution of pores, specified as a plf-function with depth points (negative [cm]) and the fraction of the pores ending at the given depth. The first point should indicate the depth of the deepest macropore and be combined with "1", and the last point should be the depth of the shallowest macropore and be combined with "0". It is assumed that the pores start at the surface. By default, the macropores extend from the top to 80-100 cm depth. In this interval, there is a linear decrease in the amount (from all pores active (1) to no pores active (0). The depth at which the macropores start and end can also be specified using optional parameters. In addition, the pressure, where macropore flow starts and where it ends can be specified (default -3 and -30 [cm], respectively), together with a ponding height, above which the water spills into macropores. This solution was default for all soils where the combined amount of humus and clay is above 5 %.

4.8 Root water uptake

Root water uptake is calculated as a steady-state flow towards the root surface applying the following assumptions (Hansen and Abrahamsen, 2009):

1. The root extracts water from a cylindrical soil volume around it and the radius of this volume corresponds to half the average distance between the roots.
2. Flow towards the root is radial and can be described by the Darcy equation.
3. The pressure potential at the outer boundary of the considered soil cylinder equals the bulk pressure potential as obtained from the solution to Richard's equation (Eq. 34 and 36).
4. The potential drop towards the root surface can be approximated by a series of steady-state profiles.
5. The plant determines the pressure potential at the root surface; however, this potential is limited by the permanent wilting point.
6. At the root surface a contact resistance exist, which can be evaluated according to Herkelrath et al. (1977).

Based on these assumptions, root water uptake, Γ_{RWU}, can be calculated as:

$$\Gamma_{RWU} = 4\pi L_{ro} \frac{\theta_{ro}}{\theta_s} \frac{M(h_p) - M(h_{ro})}{-ln(r_{ro}^2 \pi L_{ro})} \quad (39)$$

where:

L_{ro} = root density [cm cm^{-3}], calculated from root biomass and specific root length.

θ_{ro} = soil water content corresponding to the soil water at h_{ro} [cm^3 cm^{-3}],

h_{ro} = pressure potential at the root surface [cm],

r_{ro} = root radius [cm] and,

M = matrix flux potential which is a function of the pressure potential in the soil cylinder, from which the root is assumed to draw water, given by:

$$M(hp) = \int_{-\infty}^{h} K dh \quad (40)$$

where:

K = the hydraulic conductivity, and

h = the pressure potential at the outer boundary of the cylindrical soil volume, from which the root is assumed to draw water.

Two different situations for transpiration can occur: transpiration at potential rate and transpiration at a lower rate than potential.

Transpiration at potential rate

When transpiration takes place at potential rate, $E_{p,surf}$ (section 3.3), h_{ro} is calculated based on the assumption that an unknown pressure potential, ψ_x, exist at the transition between root and shoot. Based on this pressure potential, ψ_x, the pressure potential at the root surface is calculated as:

$$h_{ro} = \psi_x + (1 + R_x) \cdot z \quad (41)$$

where:

R_x = a vertical transport resistance coefficient [-] (default =10),

z = is the vertical coordinate (with 0 at the surface and positive upwards) [cm], and

ψ_x = an unknown pressure potential that is assumed to exist at the transition between root and shoot. ψ_x (and h_{ro}) is found by iteration so the following condition is fulfilled:

$$E_t = \int_0^{z_r} \Gamma_{RWU} dz \quad (42)$$

where:

E_t = the transpiration rate of the crop [cm^3 h^{-1}], and

z_r = the rooting depth [cm].

Transpiration at a lower rate than potential.

When transpiration is limited by the soil water potential, it is assumed that a common pressure exists along the root and that both ψ_x and h_{ro} can be approximated by the wilting point (h_{wp}, by default -15000 [cm]). Eq. 39 can then be solved directly.

4.9 Water flow under frost and thaw condition

When the soil temperature gets below 0 °C (chapter 5) the water in the soil starts to freeze. It is assumed that the formation of ice first takes place in the large pores, resulting in movement of water from the smaller to the larger pores. This lowers the pressure potential in the freezing soil, which results in upwards movement of water from beneath the freezing soil. Thus, water in the warmer subsoil is moving upwards to the freezing front.

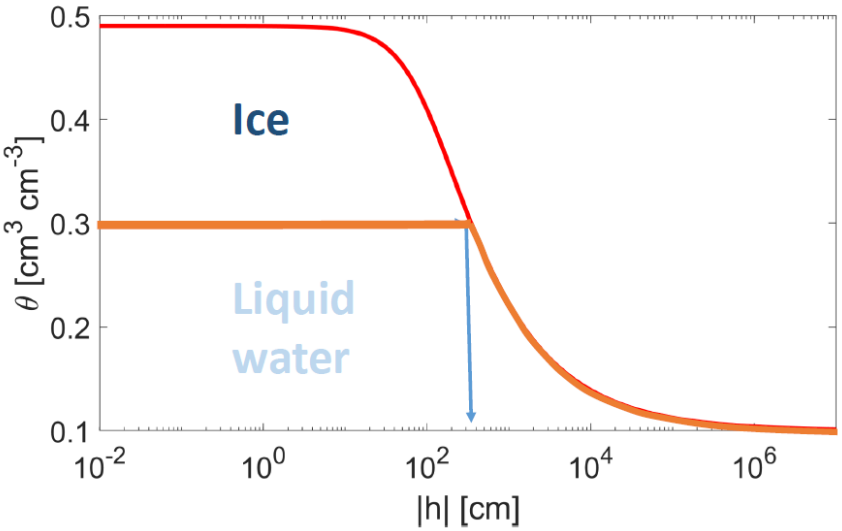

Figure 4.4. Illustration of how ice formation influences the effective retention curve. In this case, the volume above a water content of 0.3 is filled with ice, and the big pores within this volume are removed from the retention curve. Illustration by E.Diamantopoulos.

When water freezes it expands, which together with the above-described water movement, results in lower air content in the soil. However, as long as air is still present within the soil, it is assumed that the pressure potential can be found from the content of liquid water by use of the soil water retention curve.

As the ice content of the soil increases, the amount of liquid water required to establish a positive or zero pressure potential in the soil decreases, as it is assumed that ice occupies the larger pores in the soil. When the pressure potential in a freezing zone becomes zero or positive, the numerical procedure used to solve Richards Equation (Eq. 33 and 35) is no longer feasible. Thus, water movement in the freezing zone is calculated as:

$$\frac{\partial \theta}{\partial t} = \frac{\partial K_z(h_{liq})}{\partial z} + \Gamma_{RWU} + \Gamma_{DF} + \Gamma_{BF} \quad (43)$$

where $K_z(h_{liq})$ denotes the vertical hydraulic conductivity estimated for the liquid water content present in the soil based on the soil water retention and hydraulic conductivity curves (section4.5). This procedure is applied until the freezing zone thaws and air again can enter the soil.

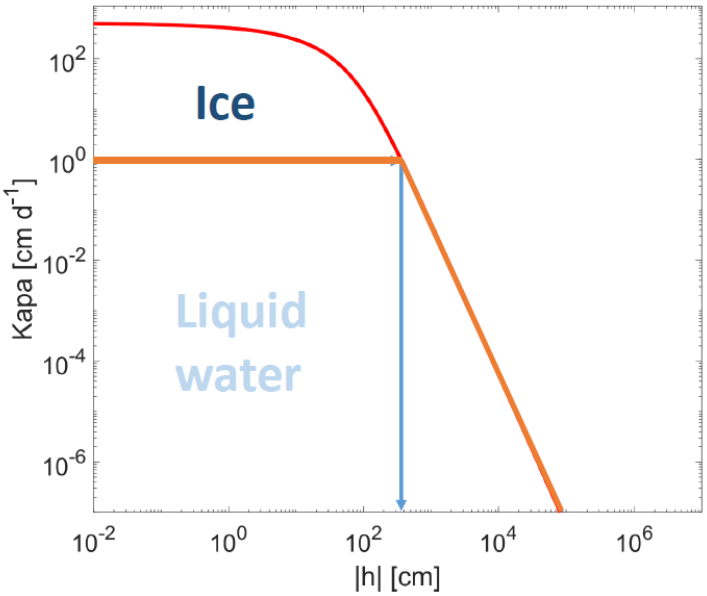

Figure 4.5. Illustration of the change in apparent hydraulic conductivity due to ice formation. As the large pores are filled with ice, only the smaller pores contribute to the hydraulic conductivity. Illustration by E.Diamantopoulos.

Below the freezing zone, in the unfrozen soil, water flow is calculated with Richard's equation (Eq. 1 and 3) by applying a specified flux at a specified depth (the border between the frozen and non-frozen zone) as upper boundary condition (section 4.4.1).

4.10 Numerical solutions

4.10.1 1-dimensional numerical solution

Richard's equation is solved numerically using a finite difference scheme in the mixed formulation (Celia et al., 1990). For details, see section 4.9 in (Hansen et al., 1990), available here.

4.10.2 2-dimensional numerical solution

Richard's equation is solved numerically using a finite volume scheme. For details see the report: Num2D-v2, section 1.3, available here.

4.11 Parameter overview

Table 4.4. Related Parameter names in Daisy.

Name and explanation		**Model (in Daisy)**	**Parameter name** ***(Daisy reference manual)***	**Default**	**Default unit**
1D discretization	array	Vertical	z_{plus}	Has default values, see section 4.1.	[cm]
2D vertical discretization	array	Rectangle	z_{plus}	User specified	[cm]
2D horizontal discretization	array	Rectangle	x_{plus}	User specified	[cm]
Clay	Fraction of clay in soil. Definition of particles size depends on which soil classification scheme is used (see Table 4.1)	horizon	*clay*	User specified	[fraction]
Silt	Fraction of silt in soil. Definition of particles size depends on which soil classification scheme is used (see Table 4.1)). Can be divided into fine, medium, and coarse.	horizon	*silt*	User specified	[fraction]
Sand	Fraction of sand in soil. Definition of particles size depends	horizon	*sand*	User specified	[fraction]

Name and explanation		Model (in Daisy)	Parameter name *(Daisy reference manual)*	Default	Default unit
	on which soil classification scheme is used (see Table 4.1)). Can be divided into very fine, fine, medium, coarse, and very coarse.				
humus	Humus content of the soil.	horizon	*humus*	User specified	[fraction]
chalk	Chalk content of the soil	horizon	*Chalk*	User specified	[fraction]
other	Typically, larger mineral components (stones, pebbles).	horizon	*Other*	User specified	[fraction]
Bulk density	Dry bulk density of the soil	horizon	*Dry_bulk_density*	User specified or calculated	[g cm^{-3}]
θ_s	Volumetric soil water content at saturation.	Hydraulic	*Theta_sat*	User specified (or given by PTFs: HYPRES and Cosby).	[fraction] [$cm^3\ cm^{-3}$]
θ_r	Residual volumetric soil water content.	Hydraulic	*Theta_res*	Generally, default = 0. However, in HYPWEB, default=0.01.	[fraction]
h_b	Bubbling pressure, air-entry value.	Hydraulic	*h_b*	User specified (or given by PTF: Cosby)	[cm]
λ	Brooks and Corey shape parameter. Poresize index.	B_BaC, M_BaC	*lambda* p		[-] [-]

Name and explanation		**Model (in Daisy)**	**Parameter name** ***(Daisy reference manual)***	**Default**	**Default unit**
p	Shape parameter for hydraulic conductivity curves		***p***	User specified or calculated, see section 4.5.	
b	Campbell shape parameter.	B_C, M_C	*b*	User specified (or given by PTF: Cosby)	[-]
α	Van Genuchten shape parameter	B_vG, M_vG	*alpha*	User specified (or given by PTF: HYPRES)	[cm^{-1}]
n	Van Genuchten shape parameter	B_vG, M_vG	*n*	User specified (or given by PTF: HYPRES)	
"l"	Tortuosity parameter	Hydraulic	*l*	Default depending on model. B_BaC, B_C, B_vG : 2 M_BaC, M_C, MvG: 0.5 (or given by PTF: HYPRES)	[-]
K_s	Saturated hydraulic conductivity	Hydraulic	*Ks*	All hydraulic conductivity models	[cm h^{-1}]
anisotropy	Horizontal saturated water conductivity relative to vertical saturated water conductivity.	horizon	*anisotropy*	1	[-]
	Static groundwater level given as a negative number below surface.	Groundwater fixed	*table*	User specified	[cm]

Name and explanation		Model (in Daisy)	Parameter name *(Daisy reference manual)*	Default	Default unit
	Data describing a varying groundwater table.	Groundwater file	*file*	Name of file to read data from. File must be structured as YEAR MONTH DAY HEIGHT	HEIGHT [groundwater level given as cm above soil surface)
	Offset to add to datapoint from *file*.	Groundwater file	*offset*	Default 0	[cm]
	Constant flux to the groundwater.	Groundwater flux	*flux*	User defined	[cm h^{-1}]
K_a	Conductivity of the aquitard.	Groundwater Aquitard	*K_aquitard*	Default 0.001	[cm h^{-1}]
Δz_a	Height of the aquitard.	Groundwater Aquitard	*Z_aquitard*	Default 200	[cm]
h_a	Pressure potential in the aquifer at the interphase between the aquitard and the aquifer.	Groundwater Aquitard	*h_aquitard*	Optional. As default equal to z_aquitard.	[cm]
	Height of groundwater that corresponds to the pressure in the aquifer.	Groundwater Aquitard	*pressure_table*	Optional.	[cm]
	Depth of soil layer where both upward and downward water	lr (uzrect)	*z_top*	-10	[cm]

Name and explanation		Model (in Daisy)	Parameter name *(Daisy reference manual)*	Default	Default unit
	movement is calculated.				
	Pressure at field capacity.	lr (uzrect)	*h_fc*	-100	[cm]
	Constant steady state water flow in horizontal direction.	const (uzrect)	*q_x*	0	[cm h^{-1}]
	Constant steady state water flow in upward vertical direction.	const (uzrect)	*q_z*	0	[cm h^{-1}]
L	Distance between drainpipes.	Drain Lateral	*L*	Default 1800	[cm]
Δx	Horizontal distance between soil column and nearest drainpipe.	Drain Lateral	*x*	Default ½L	[cm]
r	Inner radius of drainpipe.	Drain Lateral	*rad*	Default 3.5	[cm]
	Current ground water level	Drain Lateral	*height*	Optional parameter	
	Water table in drain pipe outlet.	Drain Lateral	*pipe_outlet*	By default, "*deep*", identical to pipe_position, equal to free flow. Can vary over time, see ref. manual for options under "*depth*".	[cm]

Name and explanation		Model (in Daisy)	Parameter name *(Daisy reference manual)*	Default	Default unit
	Height where drainpipes are placed in the soil.	Drain Lateral	*pipe_position*	Default -110	[cm]
	Model selected for calculation of equivalent depth for Hooghoud's equation.	Drain Lateral	*eq_depth*	*MolenWesseling*	
	Horizontal conductivity in saturated soil	Drain Lateral	*k_to_pipes*	Optional parameter. By default calculated from the hydrological conductivity and the anisotropy of the horizon.	[cm h^{-1}]
	Current effective pipe position	Drain Lateral	*pipe_level*	Optional state variable	[cm]
h_{init}	Matrix pressure needed to activate waterflow towards biopores.	Tertiary Biopores Tertary old (macro)	*pressure_initiate*	Default -3	[cm]
h_{term}	Matrix pressure needed to deactivate waterflow towards biopores.	Tertiary Biopores Tertary old (macro)	*pressure_end*	Default -30	[cm]
	Maximum height of ponding water before	Tertiary Biopores Tertary old (macro)	*pond_max*	Default 0.05	[cm]

Name and explanation		Model (in Daisy)	Parameter name *(Daisy reference manual)*	Default	Default unit
	infiltrating to biopores.				
	Pressure difference needed between matrix and biopores for water movement to and from biopores.	Tertiary Biopores	*pressure_barrier*	Default 5	[cm]
z_{top}	The height where biopore starts	Biopore old	*height_start*	User defined Optional parameter	[cm]
z_{bot}	The height where biopores end	Biopore old	*height_end*	User defined Optional parameter	[cm]
$D_{b,c}$	Biopore density, combined, eq. (45, 46)	Biopore	*density*	User defined	[biopores cm^{-2}]
r_b	Radius of the biopore, eq. (45, 46)	Biopore	*Diameter* (2*radius)	User defined	[cm]
K_w	Relative conductivity of the biopore wall compared to matrix, Eq (48)	Biopore matrix	*K_wall_relative*	User defined	[-]
	Distribution of macropore end points as a function of height	Tertary old	*distribution*	User defined, default is pores from the top to 80-100 cm depth, the amount decreasing linearly, for all soils with humus%+clay%≥ 5%	

Name and explanation		Model (in Daisy)	Parameter name *(Daisy reference manual)*	Default	Default unit
r_{ro}	Radius of roots, eq. (49)	Rootsystem	*rad*	Default 0.005	[cm]
h_{wp}	Matrix potential at wilting point	Rootsystem	*h_wp*	Default: 15000	[cm]
R_x	Transport resistance in the xylem, eq. (51)		*Rxylem*	Default: 10	[ ]

Original text from	A10, Holbak et al. (2021)	
Updated by	date	For Daisy version
Holbak, M. & Styczen, M.	2024 04 17	6.41

4.12 Appendices

4.1: Additional hydraulic functions.

4.2: Options for calculation of equivalent depth in Hooghoudt's equation.

4.13 References

Brooks, R.H., Corey, A.T., 1964. Hydraulic properties of porous media, in: Hydrology Paper No. 3. Colorado State University, Fort Collings, p. 27.

Burdine, N.T., 1953. Relative Permeability Calculations From Pore Size Distribution Data. Journal of Petroleum Technology 5, 71–78. https://doi.org/10.2118/225-G

Campbell, G.S., 1974. A Simple Method for Determining Unsaturated Conductivity From Moisture Retention Data. Soil Science June 1974, 311–314.

Celia, M.A., Bouloutas, E.T., Zarba, R.L., 1990. A general mass-conservative numerical solution for the unsaturated flow equation. Water Resources Research 26, 1483–1496. https://doi.org/10.1029/WR026i007p01483

Cosby, B.J., Hornberger, G.M., Clapp, R.B., Ginn, T.R., 1984. A Statistical Exploration of the Relationships of Soil Moisture Characteristics to the Physical Properties of Soils. Water Resources Research 20, 682–690. https://doi.org/10.1029/WR020i006p00682

Hansen, S., Abrahamsen, P., 2009. Modeling water and nitrogen uptake using a single-root concept: Exemplified by the use of the Daisy model, in: Quantifying and Understanding Plant Nitrogen Uptake for Systems Modeling. CRC Press, Taylor & Francis Group, pp. 169–196.

Hansen, S., Jensen, H.E., Nielsen, N.E., Svendsen, H., 1990. DAISY - Soil Plant Atmosphere System Model, NPo-forskning fra Miljøstyrelsen. Miljøstyrelsen, Strandgade 29, 1401 København K.

Hansen, S., Petersen, C.T., Mollerup, M., Abrahamsen, P., Gjettermann, B., Nielsen, M.H., Styczen, M.E., Poulsen, R., Lørup, J.K., Yamagata, K., Butts, M.B., 2012. Flerdimensional modellering af vandstrømning og stoftransport i de øverste 1–2 m af jorden i systemer med markdræn. Miljøstyrelsen.

Herkelrath, W.N., Miller, E.E., Gardner, W.R., 1977. Water Uptake By Plants: II. The Root Contact Model. Soil Science Society of America Journal 41, 1039–1043. https://doi.org/10.2136/sssaj1977.03615995004100060004x

Holbak, M., Abrahamsen, P., Hansen, S., Diamantopoulos, E., 2021. A physically based model for preferential water flow and solute transport in drained agricultural fields. Water Resources Research 57, e2020WR027954. https://doi.org/10.1029/2020WR027954

Hooghoudt, S.B., 1940. Bijdragen tot de kennis van eenige natuurkundige grootheden van den grond: Algemeene beschouwing van het probleem van de detailontwatering en de infiltratie door middel van parallel loopende drains, greppels, slooten en kanalen.

Mollerup, M., Abrahamsen, P., Petersen, C.T., Hansen, S., 2014. Comparison of simulated water, nitrate, and bromide transport using a Hooghoudt-based and a dynamic drainage model. Water Resources Research 50, 1080–1094. https://doi.org/10.1002/2012WR013318

Mollerup, M., Hansen, S., 2007. Power series solution for falling head ponded infiltration with evaporation. Water Resources Research 43. https://doi.org/10.1029/2006WR004928

Mualem, Y., 1976. A new model for predicting the hydraulic conductivity of unsaturated porous media. Water Resour. Res. 12, 513–522. https://doi.org/10.1029/WR012i003p00513

Richards, L.A., 1931. Capillary conduction of liquids through porous mediums. Physics 1, 318–333. https://doi.org/10.1063/1.1745010

Smith, R.E., 1992. OPUS: An Integrated Simulation Model for Nonpoint-Source Pollutants at the Field Scale., Agricultural Research Service. Department of Agriculture (USA).

Tofteng, C., Hansen, S., Jensen, H.E., 2002. Film and Pulse Flow in Artificial Macropores. Hydrology Research 33, 263–274. https://doi.org/10.2166/nh.2002.0007

Tokunaga, T.K., 2009. Hydraulic properties of adsorbed water films in unsaturated porous media. Water Resources Research 45. https://doi.org/10.1029/2009WR007734

van der Molen, W.H., Wesseling, J., 1991. A solution in closed form and a series solution to replace the tables for the thickness of the equivalent layer in Hooghoudt's drain spacing formula. Agricultural Water Management 19, 1–16. https://doi.org/10.1016/0378-3774(91)90058-Q

Van Genuchten, M.T., 1980. A closed-form equation for predicting the hydraulic conductivity of unsaturated soils. Soil science society of America journal 44, 892–898.

Weber, T.K.D., Durner, W., Streck, T., Diamantopoulos, E., 2019. A modular framework for modelling unsaturated soil hydraulic properties over the full moisture range. Water Resour. Res. 2018WR024584. https://doi.org/10.1029/2018WR024584

Weber, T.K.D., Finkel, M., Gonçalves, M. da C., Vereecken, H., Diamantopoulos, E., 2020. Pedotransfer Function for the Brunswick Soil Hydraulic Property Model and Comparison to the van Genuchten-Mualem Model. Water Resources Research 56, e2019WR026820. https://doi.org/10.1029/2019WR026820

Wösten, J.H.M., Lilly, A., Nemes, A., Le Bas, C., 1998. Using existing soil data to derive hydraulic parameters for simulation models in environmental studies and in land use planning. Report.